

Efficient CRISPR/Cas12a-Based Genome-Editing Toolbox for Metabolic Engineering in *Methanococcus maripaludis*

Jichen Bao, Enrique de Dios Mateos, and Silvan Scheller*

Cite This: *ACS Synth. Biol.* 2022, 11, 2496–2503

Read Online

ACCESS |



Metrics & More



Article Recommendations

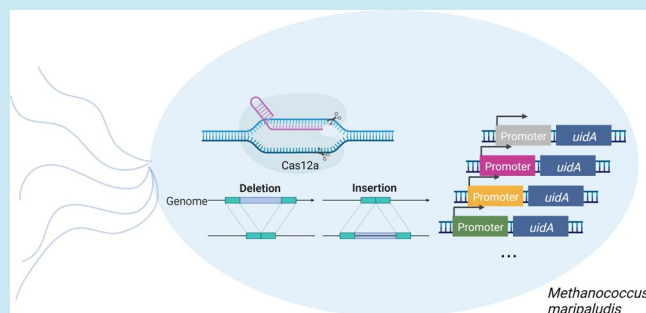


Supporting Information

ABSTRACT: The rapid-growing and genetically tractable methanogen *Methanococcus maripaludis* is a promising host organism for the biotechnological conversion of carbon dioxide and renewable hydrogen to fuels and value-added products. Expansion of its product scope through metabolic engineering necessitates reliable and efficient genetic tools, particularly for genome edits that affect the primary metabolism and cell growth. Here, we have designed a genome-editing toolbox by utilizing Cas12a from *Lachnospiraceae* bacterium ND2006 (LbCas12a) in combination with the homology-directed repair machinery endogenously present in *M. maripaludis*. This toolbox can delete target genes with a success rate of up to 95%, despite the hyperpolyploidy of *M. maripaludis*.

For the purpose of demonstrating a large deletion, the *M. maripaludis* flagellum operon (~8.9 kbp) was replaced by the *Escherichia coli* β -glucuronidase gene. To facilitate metabolic engineering and flux balancing in *M. maripaludis*, the relative strength of 15 different promoters was quantified in the presence of two common growth substrates, either formate or carbon dioxide and hydrogen. This CRISPR/LbCas12a toolbox can be regarded as a reliable and quick method for genome editing in a methanogen.

KEYWORDS: *Methanococcus maripaludis*, methanogens, CRISPR/Cas12a, genome editing, metabolic engineering, synthetic biology



INTRODUCTION

Methanogenic archaea are biotechnologically employed in a variety of uses, e.g., for methane production in anaerobic digestors,¹ as biocatalysts in power-to-gas processes,² and as versatile hosts for the development of synthetic pathways that convert carbon dioxide (CO₂) into value-added products.^{3,4} Hydrogenotrophic methanogens utilize the reductive acetyl-CoA pathway for CO₂ fixation,⁵ an energy-efficient route to synthesize organic carbon from CO₂ and hydrogen (H₂), which is similar to that found in acetogens.⁶ Subtle differences exist between the acetogenic⁷ and methanogenic CO₂ reduction pathways in terms of ATP investment and cofactor utilization.⁸ Depending on the type of product that needs to be generated from CO₂ as the carbon source, methanogens may be better-suited hosts than acetogens. Recently, the methanogen *Methanosarcina acetivorans* was re-engineered to no longer depend on methane production for its energy metabolism,⁹ thereby serving as an example where a methanogen could be utilized for generating an expanded repertoire of new potential products besides methane.

Methanococcus maripaludis is a promising methanogenic host organism for metabolic engineering of CO₂-fixation pathways due to its advantageous growth properties, e.g., 2 h doubling time,^{10,11} moderate growth temperature of 38 °C, and ability to fix nitrogen.^{12–14} Typical electron donors for CO₂ reduction in *M. maripaludis* include formate, H₂, and bioelectrically

coupled systems.^{15,16} Efforts to expand the product scope of *M. maripaludis* beyond methane are already underway. As an example, the mevalonate pathway in this methanogen was metabolically engineered to produce geraniol from CO₂ and formate.⁴ Efficient and reliable genome-editing tools are critical for successful metabolic engineering in *M. maripaludis*. Marker recycling is a prerequisite for multitarget engineering. In the case of *M. maripaludis*, while a pop-in/pop-out markerless-based genome-editing technique has been developed,¹⁷ it tends to have a problematic low positive rate, which can sometimes be less than 5%,¹⁷ particularly for those modifications that affect cell growth. As an alternative, the CRISPR/Cas (clustered regularly interspaced short palindromic repeats/CRISPR associated protein) system might remedy this problem because of its reputation for highly efficient genome editing.

The CRISPR/Cas9 system has already been successfully used for genome editing in a variety of organisms^{18–23} owing to its simplicity and high efficiency, but only a few CRISPR

Received: March 16, 2022

Published: June 22, 2022



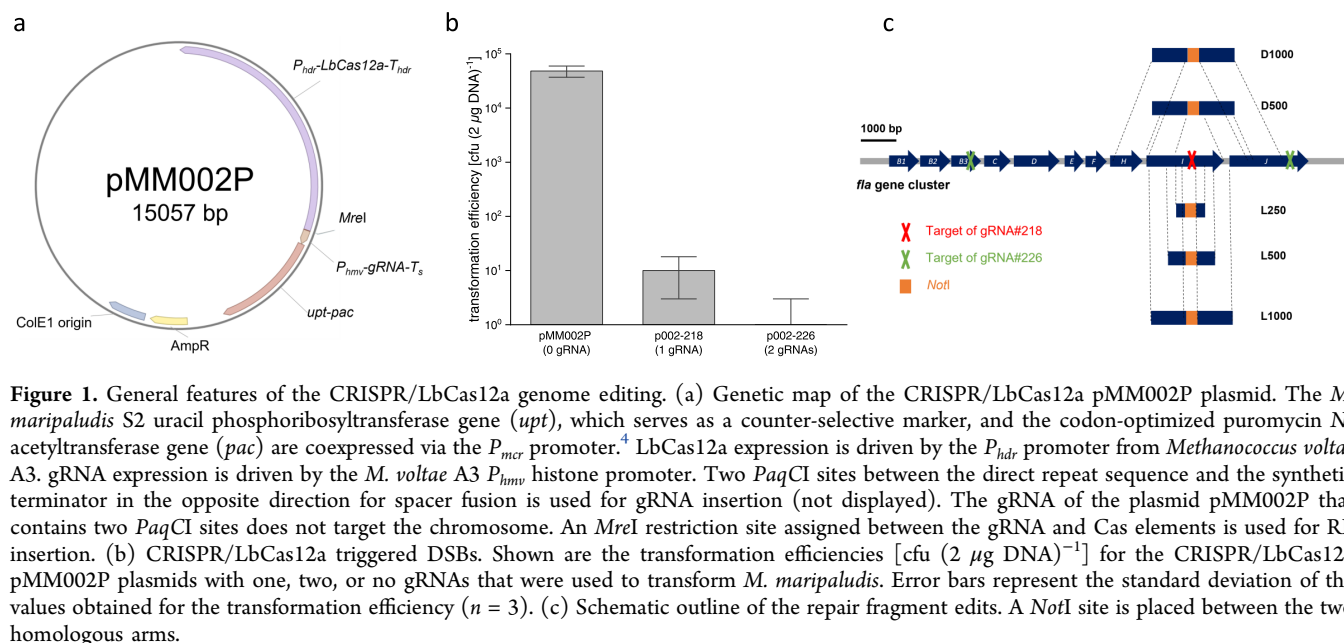


Figure 1. General features of the CRISPR/LbCas12a genome editing. (a) Genetic map of the CRISPR/LbCas12a pMM002P plasmid. The *M. maripaludis* S2 uracil phosphoribosyltransferase gene (*upt*), which serves as a counter-selective marker, and the codon-optimized puromycin *N*-acetyltransferase gene (*pac*) are coexpressed via the P_{mcr} promoter.⁴ LbCas12a expression is driven by the P_{hdr} promoter from *Methanococcus voltae* A3. gRNA expression is driven by the *M. voltae* A3 P_{hmv} histone promoter. Two *Paq*CI sites between the direct repeat sequence and the synthetic terminator in the opposite direction for spacer fusion is used for gRNA insertion (not displayed). The gRNA of the plasmid pMM002P that contains two *Paq*CI sites does not target the chromosome. An *Mre*I restriction site assigned between the gRNA and Cas elements is used for RF insertion. (b) CRISPR/LbCas12a triggered DSBs. Shown are the transformation efficiencies [cfu ($2 \mu\text{g DNA}$)⁻¹] for the CRISPR/LbCas12a pMM002P plasmids with one, two, or no gRNAs that were used to transform *M. maripaludis*. Error bars represent the standard deviation of the values obtained for the transformation efficiency ($n = 3$). (c) Schematic outline of the repair fragment edits. A *Not*I site is placed between the two homologous arms.

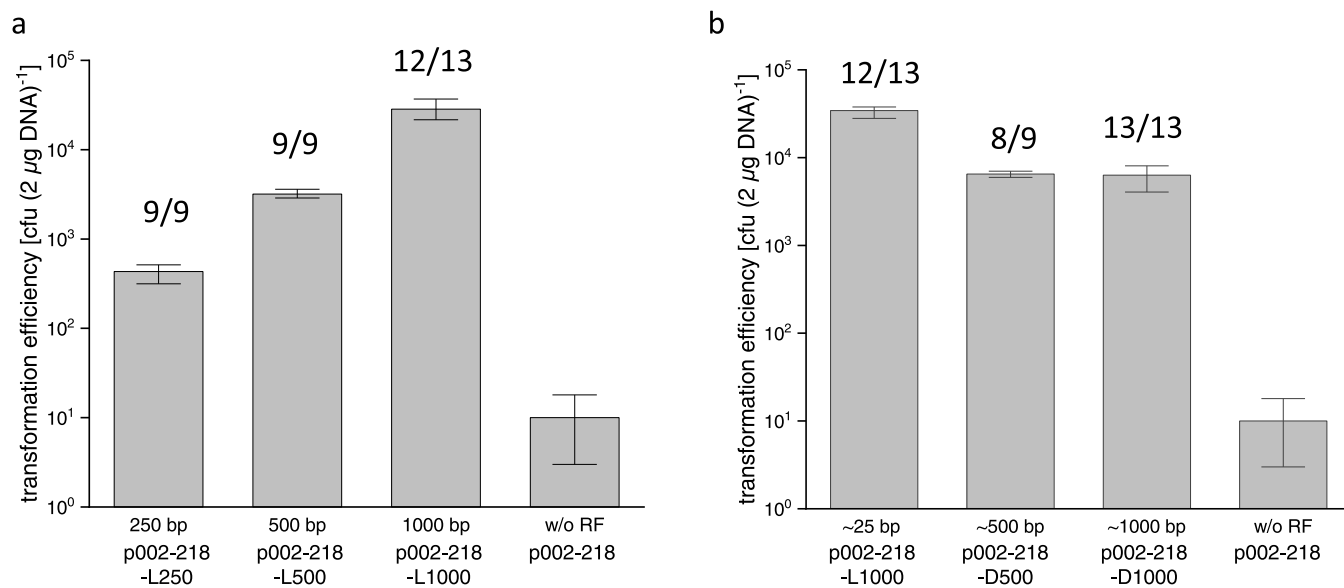


Figure 2. Effect on transformation and genome-editing (positive rates) efficiencies when the length and position of the RF are modified. Transformation efficiency and positive rate in relation to the length and position of the RF. Shown are the transformation efficiencies [cfu ($2 \mu\text{g DNA}$)⁻¹] for the CRISPR/LbCas12a pMM002P-derived plasmids that were used to transform *M. maripaludis*. (a) CRISPR/LbCas12a plasmid p002-218, in which the lengths of the homology arms flanking the RF are 250, 500, and 1000 bp (p002-218-L250, p002-218-L500, and p002-218-L1000, respectively). The distance from the RF to DSB for all plasmids is ~ 25 bp. (b) CRISPR/LbCas12a plasmid p002-218 with 1000 bp homologous arms, in which the distance between the RF and the DSB is ~ 25 , ~ 500 , and ~ 1000 bp (p002-218-L1000, p002-218-D500, and p002-218-D1000, respectively). p002-218 without the RF is included as a control. Error bars represent the standard deviation of the values obtained for the transformation efficiency ($n = 3$). Positive rates representing the fraction of correctly edited colonies per colonies tested by PCR are shown for all plasmid transformations (numbers above bars).

genome-editing toolboxes have been developed for archaea.²⁴ The first CRISPR/Cas9-mediated genome-editing system for a methanogen was reported in 2017 using *M. acetivorans* as the model organism.²⁵ This Cas9-based system recognizes and cleaves a 20-nucleotide target sequence that is flanked by a 3'-NGG protospacer adjacent motif (PAM). This contrasts with Cas12a, which instead recognizes the 5'-thymine (T)-rich PAM 5'-TTTV. This recognition site makes Cas12a the better option for developing a CRISPR toolbox in microbes with an adenine (A)- and T-rich genome. Another advantageous

attribute of Cas12a lies in its ribonuclease activity, which allows the formation of multiple guide RNAs (gRNAs) from a single transcript.^{26,27} Since the *M. maripaludis* genome has a high AT content (67.1%), we decided to use the Cas12a from *Lachnospiraceae bacterium* ND2006 (LbCas12a) and combine it with the intrinsic homology-directed repair machinery to develop a CRISPR genome-editing toolbox. In our study, we examined how the length of the repair fragment (RF) and the distance of the RF to the double-stranded break (DSB) impact on the genome-editing efficiency. As an application of our

toolbox, we deleted the *M. maripaludis* flagellum operon and replaced it with the *Escherichia coli* β -glucuronidase gene. To further expand the versatility and editing potential of this genetic toolbox, we also established a Cas9-based editing system, and we quantified the relative strength of 15 different promoters in the presence of two common growth substrates, either formate or H₂ and CO₂.

RESULTS AND DISCUSSION

CRISPR/Cas12a-Based Introduction of Double-Stranded Breaks and Transformation Efficiency. For this study, we utilized the host strain *M. maripaludis* JJ Δ upt in all experiments as well as a recently established natural transformation protocol.²⁸ The *E. coli*/*M. maripaludis* shuttle vector pLW40²⁹ served as the backbone for constructing the final toolbox plasmid pMM002P (Table S1). Further details about pMM002P and its construction are given in Figure 1a. The transformation efficiency of pMM002P into JJ Δ upt cells was calculated to be about 5×10^4 colony forming units per 2 μ g DNA [cfu (2 μ g DNA)⁻¹] (Figure 1b), which was similarly obtained for pMM001 (pMM002P lacking LbCas12a) (data not shown). The high transformation efficiency suggests that LbCas12a expression is not toxic in *M. maripaludis*. Because the coexpression of LbCas12a with either one or two gRNA sequences resulted in only 3–18 and 0–3 transformant colonies, respectively (Figure 1b,c), we conclude that the LbCas12a–gRNA complex can cause a lethal DSB in the *M. maripaludis* chromosome. Since nonhomologous end-joining (NHEJ) machineries for DNA repair are rare in archaea,³⁰ and as *M. maripaludis* JJ lacks a homolog of the Ku protein (which has a strong binding affinity for free DNA ends or nicks), NHEJ is not expected to provide an escape from such DSBs.

CRISPR/LbCas12a Genome Editing by Providing a Repair Fragment on the pMM002P-Derived Plasmid.

For CRISPR/LbCas12a genome editing, a gRNA was expressed on pMM002P (p002-218) that targets the *flaI* (*MMJJ_11570*) gene of the *M. maripaludis* flagellum operon. The lethal effect of the functional gRNA could be relieved by including RFs with various lengths of the homology arms (Figures 1c and 2a). A 1000 bp homology arm on either side resulted in a transformation efficiency of 2.8×10^4 cfu (2 μ g DNA)⁻¹. We therefore used homology arms of this length for all subsequent experiments. While 250 bp homology arms were long enough to repair DSBs created by the Cas12a/gRNA complex, the transformation efficiency was 70 times lower. We also examined what effect the distance between the RF and the DSB would have on the transformation efficiency by testing three different distances (i.e., ~25, ~500, and ~1000 bp) (Figures 1c and 2b). The transformation efficiency was found to be five times lower with the 500 bp distance than with the 25 bp distance (two-sided *t*-test, $P < 0.001$), but no significant difference was observed whether 500 or 1000 bp distances were used (two-sided *t*-test, $P > 0.05$). Because *M. maripaludis* contains an active *PstI* restriction modification system, cells are able to digest foreign DNA containing unmethylated *PstI* sites, which lowers the transformation efficiency by 1.6–3.4 fold per *PstI* site.³¹ This reduction of the transformation efficiency is exemplified by the presence of one *PstI* site in each of the 500 and 1000 bp homology arms, as any restriction digestion would likely be responsible for a lower number of transformants (Figure 2b). The similar transformation efficiency obtained with the 500 and 1000 bp distances to the DSB suggests that the genome-editing efficiency is unaffected within

a distance length of 1000 bp. To assess the positive rate of genome editing, two sets of primers were used to amplify a DNA sequence on both sides of the homology arms on the chromosome. Each of the PCR products was then subjected to *NotI* digestion. Here, a *NotI* restriction site was engineered between the left and right RFs, so that the wild-type polyploid genome copies are distinguishable from the edited ones (Figure 1c). The PCR products were sequenced afterward to confirm that the sites were edited as expected. As a result, genome editing was highly efficient, displaying a positive rate of 89–100% (Figure 2a). All results taken together (see Figure 2), 63 out of 66 colonies had been correctly edited, which equates to an average positive rate of nearly 95%. Hence, we conclude that our CRISPR/LbCas12a toolbox can reliably perform genome editing in *M. maripaludis* (see the Supporting information for a detailed description of the general procedure for utilizing the CRISPR/LbCas12a genome-editing toolbox in *M. maripaludis*).

CRISPR/LbCas12a Genome Editing by Providing a Repair Fragment Separately. To help speed up the construction of different genome-edited mutants in parallel, we modified our CRISPR/LbCas12a toolbox by providing the RF separately as a suicide plasmid. For this alternative procedure, the CRISPR/LbCas12a cleavage plasmid was cotransformed with a suicide plasmid containing a promoter–*uidA* fusion expression cassette (for further details, see the section below on promoter strengths) flanked on either side by 1000 bp homology arms. While we successfully obtained transformants with this modification, the transformation efficiency was lowered by 10–50 fold, but the genome-editing efficiency was robust and remained high. As proof, when we randomly selected and examined three transformants from the 15 different genome-edited constructs made using the suicide plasmid, all of them (45/45) were found to be positive (data not shown). We also examined the possibility of cotransforming the CRISPR/LbCas12a cleavage plasmid with the RF separately by providing it as a linear PCR product. In this case, while genome editing was deemed successful, the transformation efficiency was 100–1000 times lower than that obtained using our original CRISPR/LbCas12a toolbox method with the plasmid containing the 1000 bp homology arm (p002-218-L1000).

Using CRISPR/LbCas12a Genome Editing to Replace a Large Genome Fragment with a Heterologous Gene.

As an application of our CRISPR/LbCas12a method, we demonstrated its use as a tool for heterologous gene integration. We removed the entire ~8.9 kbp flagellum operon (*flaB1B2B3CDEFGHIJ MMJJ_11660* – *MMJJ_11560*) from the *M. maripaludis* chromosome and substituted it with the *E. coli* β -glucuronidase gene (*uidA*). This edit was performed using two different CRISPR/LbCas12a plasmids: p002-218-*uidA*, which has one gRNA that generates a single lethal DSB on the chromosome, resulting in two long distances between the DSB and the RF (i.e., 6.4 and 2.5 kbp), and p002-226-*uidA*, which has two different gRNAs that cleave at either side of the flagellum operon and thus shorten the distances between the DSB and the RF (i.e., 0.25 and 1.6 kbp). Both plasmids resulted in a similar transformation efficiency (Figure 3), demonstrating that our CRISPR/LbCas12a method can successfully generate a large chromosomal fragment deletion. The positive rate of genome editing was lower when only one gRNA was used, as it seems the 6.4 kbp distance (Figure 3) affects the positive rate by exceeding the 1000 bp length. A

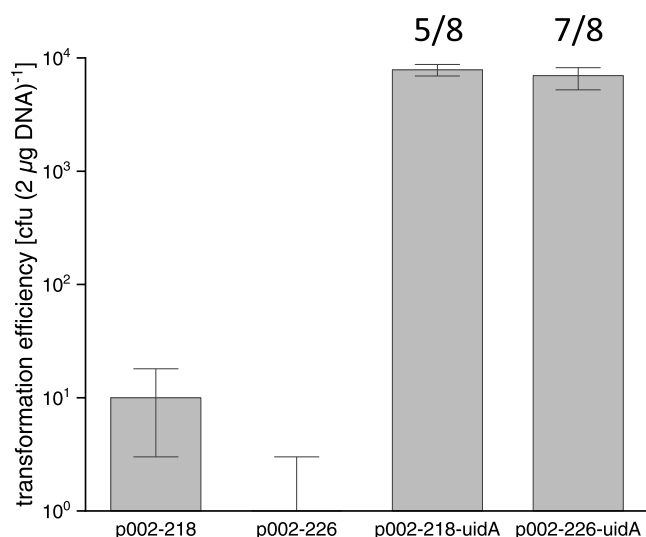


Figure 3. CRISPR/LbCas12a genome-edited replacement of the *M. maripaludis* flagellum operon with the *E. coli* β -glucuronidase gene (*uidA*). Shown are the transformation efficiencies [cfu (2 μ g DNA)⁻¹] for the CRISPR/LbCas12a pMM002P-derived plasmids that were used to transform *M. maripaludis*. Plasmids p002-218 and p002-226 (controls) express one and two gRNAs, respectively, and do not contain the RF. Plasmids p002-218-uidA and p002-226-uidA express one and two gRNAs, respectively, but contain the RF. Error bars represent the standard deviation of the values obtained for the transformation efficiency ($n = 3$). Positive rates representing the fraction of correctly edited colonies per colonies tested by PCR are shown for the p002-218-uidA and p002-226-uidA transformations (numbers above bars).

similar effect was observed for *M. acetivorans*, in which the positive rate was significantly reduced when the distance to the DSB went beyond 1000 bp.²⁵ In addition, the transformation efficiency had also decreased with an increasing distance.²⁵ Using two gRNAs to shorten the distance between the RF and the DSB might help improve the transformation and genome-editing efficiencies also in other methanogen-based CRISPR systems.

To be ready for a second round of genome editing in the future, the CRISPR plasmid was removed after genome editing by being counter-selected on a plate containing 6-azauracil. The absence of the plasmid was confirmed by the inability of the cells to grow on the medium containing puromycin, and the removal rate was 9/10.

Development of the CRISPR/SpCas9 Genome-Editing System. To expand the gRNA repertoire in our CRISPR/Cas toolbox, we also constructed a Cas9-based genome-editing plasmid that uses the *Streptococcus pyogenes* Cas9 endonuclease. With this CRISPR/SpCas9 tool, we were able to successfully replace the 1.9 kbp fragment covering the alanine dehydrogenase–alanine racemase genes (*ald-als*, MMJJ_13250 – MMJJ_13260) in the *M. maripaludis* chromosome with a 4.2 kbp DNA fragment containing a different heterologous gene. Here, the CRISPR/SpCas9 cleavage plasmid with one gRNA was cotransformed with a suicide plasmid containing the 4.2 kbp DNA fragment flanked on both sides by 1000 bp homology arms. The transformation efficiency was only 317 ± 123 cfu (2 μ g DNA)⁻¹, but the rate of genome editing was high (8/10 colonies were edited) (Figure 4). Since the RF contained two *Pst*I sites, they can explain the lower transformation efficiency of this genome-editing system.

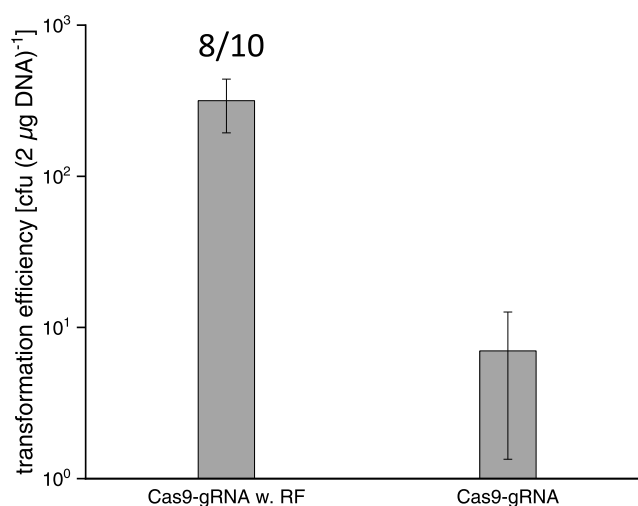


Figure 4. CRISPR/SpCas9 genome-edited replacement of the *M. maripaludis* alanine dehydrogenase–alanine racemase (*ald-als* 1.9 kbp) genes with a 4.2 kbp fragment. Shown are the transformation efficiencies [cfu (2 μ g DNA)⁻¹] for the CRISPR/SpCas9 plasmids that were used to transform *M. maripaludis*. The left bar indicates that the cells were transformed with a suicide plasmid containing the integration cassette and a CRISPR/SpCas9 plasmid carrying a gRNA targeting to the *ald-als*. The right bar indicates that the cells were only transformed with a CRISPR/SpCas9 plasmid carrying a gRNA targeting to the *ald-als*. Error bars represent the standard deviation of the values obtained for the transformation efficiency ($n = 3$). The positive rate representing the fraction of correctly edited colonies per colonies tested by PCR is shown for the transformations (numbers above the left bar).

Promoter Strengths of 15 Different Promoter–*uidA* Fusions Constructed by CRISPR/LbCas12a.

Fifteen different promoters delivered as a promoter–*uidA* fusion expression cassette were integrated into the locus of the acetyl-CoA synthetase gene (MMJJ_09370) of *M. maripaludis* JJ using the CRISPR/LbCas12a toolbox (for further details, see earlier section). Three promoters (P_{mcr_JJ} , P_{mcr_JJ} , and P_{fla_JJ}) originated from *M. maripaludis* JJ, while the remaining twelve were from the closely related methanogen, *Methanococcus vannielii* SB. The relative strengths of these promoters were measured in the presence of two common growth substrates, either formate or H₂ and CO₂. All promoters except P_{nif} and P_{hdrC1} had successfully driven the expression of *uidA* using both growth substrates (Figure 5). P_{hdrC1} had allowed gene expression in only the formate-containing growth medium, while no expression was detected for P_{nif} in both growth substrates. Since P_{mcr} is regarded as a strong constitutive promoter in methanogens,³² then by comparison, P_{glnA} , P_{mtr} , P_{mcr} , P_{mcr_JJ} , and P_{fla_JJ} can be judged as strong promoters in *M. maripaludis*. Transcription from P_{nif} is normally repressed by the nitrogen regulatory protein R (NrpR) but can become highly active when N₂ gas serves as the sole nitrogen source or else in the absence of NrpR.³³ With this in mind, we deleted the *nrpR* gene from the genome-edited P_{nif} –*uidA* strain and found that P_{nif} was no longer repressed and had instead increased in strength significantly (2670 ± 58 nmol min⁻¹ OD₆₀₀⁻¹) (two-sided *t*-test, $P < 0.001$). It is tempting to speculate that the Δ *nrpR*– P_{nif} strain might be a useful host for target genes requiring very strong

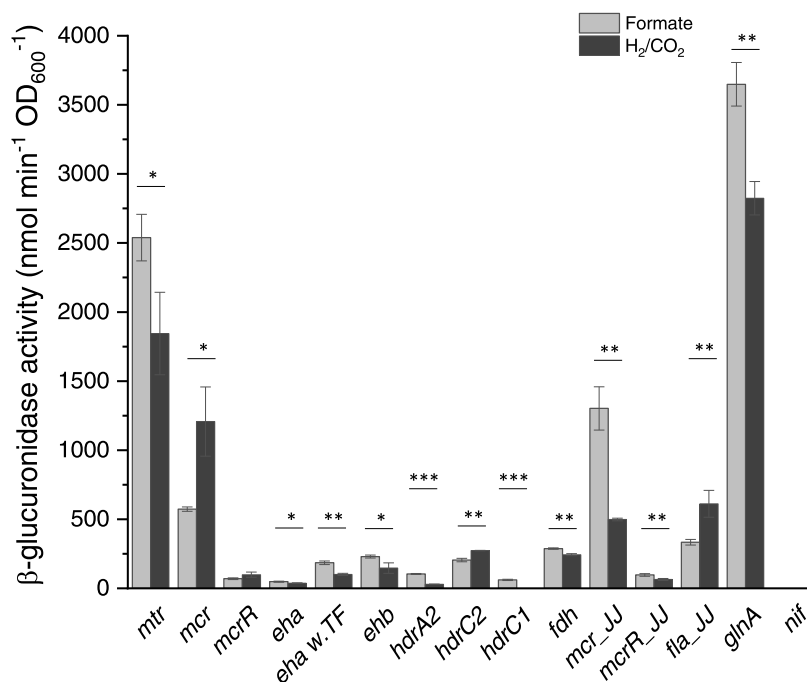


Figure 5. Quantification of promoter strengths for the two different growth conditions formate or H₂/CO₂, measured after the culture has reached OD₆₀₀ = ca. 0.5. The promoters *mcr_JJ*, *mcrR_JJ*, and *fla_JJ* are from *M. maripaludis* JJ. The remaining promoters are from *M. vannielii* SB. Error bars represent the standard deviation ($n = 3$). The activity of the *hdrC1* promoter in H₂/CO₂ medium and the *nif* promoter in formate and H₂/CO₂ medium cannot be detected. * $P < 0.05$; ** $P < 0.01$; *** $P < 0.001$.

expression. For the majority of the promoters, their strengths were similar for both growth substrates.

While P_{eha} normally drives the expression of the energy-converting hydrogenase A gene (*eha*) in *M. vannielii*, it was observed as a weak promoter in *M. maripaludis*. P_{eha} does not directly control the *eha* gene expression, but instead first drives the expression of a putative transcriptional factor (TF) gene that precedes the *eha* gene, wherein both genes are presumably part of an operon. We also examined a *uidA* construct that includes the TF gene after the $P_{eha\ w.TF}$ promoter sequence. The *uidA* expression using both growth substrates was found to be significantly higher for the $P_{eha\ w.TF}$ construct than the P_{eha} one (two-sided t -test, $P < 0.01$). These results suggest that this transcriptional factor might regulate *eha* expression. On the other hand, P_{glnA} from *M. vannielii* was unexpectedly strong in *M. maripaludis*, even with the presence of the NrpR repressor or ammonium in the growth medium. DNA sequencing of the integrated P_{glnA} -*uidA* expression cassette eliminated a possible point mutation or other change as being responsible for this unusual promoter strength. Likewise, constructing and testing a new P_{glnA} -*uidA* *M. maripaludis* strain still gave the same result. Thus, one can confidently conclude that P_{glnA} from *M. vannielii* functions as a strong promoter in *M. maripaludis*. In *M. maripaludis*, native P_{glnA} normally directs basal constitutive expression levels when ammonium is present.³⁴ Although the *glnA* operator for P_{glnA} is the same in *M. vannielii* and *M. maripaludis*, the P_{glnA} -*uidA* strain appears to have the highest promoter strength among all others tested in this study.

CONCLUSIONS

M. maripaludis already possesses several efficient genetic tools and transformation protocols for standard applications,^{17,28,31} e.g., such as the classic pop-in/pop-out genome-editing technique.¹⁷ In some instances, however, this genetic editing

tool is hindered by a low positive rate, with many colonies requiring to be screened to obtain a desired genotype, particularly when the targets to be engineered affect cell growth.³² As a solution, we have developed a reliable CRISPR/Cas12a toolbox that can efficiently knock-in or knock-out genes in *M. maripaludis* with a positive rate of at least 95%. Notably, our system requires only a single round of homologous recombination and lacks merodiploid formation, which then lowers the workload of genome editing and increases the overall success rate. The option of providing the RF separately as a suicide plasmid or PCR fragment might further speed up the genome-editing process. Since Cas12a displays ribonuclease activity that can process a single continuous multi-gRNA transcript,^{26,27} it might be convenient to express two gRNAs via our CRISPR/LbCas12a system, thus saving the time and cost of additional plasmid construction. Our CRISPR/LbCas12a toolbox can also allow for heterologous protein production in *M. maripaludis*, as it drives the stable integration of genes into the chromosome. *M. maripaludis* might become an attractive expression host for many proteins that are difficult to be produced in *E. coli*, e.g., such as formate dehydrogenase,¹⁶ methyl-coenzyme M reductase,³⁵ and heterodisulfide reductase.³⁶ While a variety of promoters have thus far been studied and used for synthetic biology in *M. maripaludis*,^{14,33,37,38} a uniform system to compare their strengths has been lacking. In that context, our CRISPR/LbCas12a genome-editing toolbox now represents a versatile system for engineering and balancing metabolic fluxes in *M. maripaludis* strains.

MATERIALS AND METHODS

Plasmids and Strains. All plasmids and strains used in this study are listed in Tables S1 and S2, respectively. Links to plasmid maps are listed in Table S3. *M. maripaludis* JJ Δ upt²⁸

and plasmid pLW40²⁹ are gifts from Prof. Kyle Costa, University of Minnesota. Plasmid pMEV4⁴ was kindly provided by Prof. William B Whitman, University of Georgia. *M. maripaludis* S2³⁹ was kindly provided by Prof. John Leigh and Dr. Thomas Lie, University of Washington. *E. coli* NEB5 α (New England Biolabs) was used for plasmid construction. The plasmids pMM002P and pMM005 were constructed by Gibson assembly.⁴⁰ The construction protocol and primers for pMM002P and pMM005 are described in Tables S4 and S5, respectively. All of the cleavage plasmids were constructed in the following manner. For LbCas12a gRNA, the forward primer consisted of 5'-AGAT and 24-nucleotide guide sequence, whereas the reverse primer consisted of 5'-TATC and 24-nucleotide reverse complement guide sequence. For SpCas9 gRNA, the forward primer consisted of 5'-AGTG and 20-nucleotide guide sequence, whereas the reverse primer consisted of 5'-AAAC and 20-nucleotide reverse complement guide sequence. Both sets of forward and reverse primers containing the gRNA and a 5' four-nucleotide overhang were annealed. The annealing product was ligated to *Paq*CI-digested pMM002P or pMM005 vector DNA. CRISPR guide sequences were designed using the CHOPCHOP webtool (<https://chopchop.cbu.uib.no/>).⁴¹ The RF was inserted into the corresponding cleavage plasmid at the *Mre*I restriction site. Additional primers used in this study are listed in Table S6.

Growth Media and Conditions. Lysogeny broth medium (10 g L⁻¹ tryptone, 10 g L⁻¹ NaCl, and 5 g L⁻¹ yeast extract) containing 50 mg L⁻¹ ampicillin was used for plasmid construction. Liquid McC medium was used for growing *M. maripaludis* strains with an anoxic headspace (2.8 bar, 80% H₂/20% CO₂).²⁸ Sealed culture tubes were incubated at 37 °C with 200 rpm agitation. McFC medium with an anoxic headspace (1 bar, 80% N₂/20% CO₂) was used when formate served as the carbon source.⁴² Sealed culture tubes were incubated statically at 37 °C. Puromycin (2.5 μ g mL⁻¹) or 6-azauracil (0.25 mg mL⁻¹) was added as required.

***M. Maripaludis* Transformation.** The natural transformation of *M. maripaludis* was performed using a previously described protocol.²⁸ Briefly, a sealed tube containing a 5 mL of *M. maripaludis* culture was grown overnight to an OD₆₀₀ between 0.7 and 1.2. Two micrograms of DNA was then added directly to the culture. This was followed by flushing the headspace with a gas mixture of 80% H₂ and 20% CO₂ for 30 s and adjusting the pressure to 2.8 bar. The sealed culture tube was then incubated at 37 °C with 200 rpm agitation for 4 h, after which the cells were spread-plated onto solid McC medium supplemented with 2.5 μ g mL⁻¹ puromycin and grown anaerobically at 37 °C.

Curing of the CRISPR/Cas Plasmid from *M. Maripaludis* Strains. *M. maripaludis* strains containing the CRISPR/Cas toolbox plasmid were grown in 5 mL of liquid McC medium without antibiotics to an OD₆₀₀ between 0.7 and 1.2. A 100 μ L aliquot of each culture was used to inoculate another 5 mL of liquid McC medium lacking antibiotics and allowed to incubate overnight. A single droplet of culture was then streaked out onto solid McC medium containing 0.25 mg mL⁻¹ 6-azauracil. After 3–5 days, several isolated colonies were selected and streaked out onto another plate of the same medium for purification of plasmid-free cells.

β -Glucuronidase Activity Measurements. 4-Nitrophenyl β -D-glucuronide (4-NPG, Sigma-Aldrich) served as the substrate and was prepared as a 10 mg mL⁻¹ stock solution in 50 mM sodium phosphate buffer, pH 7.0 (Na-PB). For

measuring β -glucuronidase activity, a tube of *M. maripaludis* cells was first grown to an OD₆₀₀ of \sim 0.5 (BioPhotometer plus, Eppendorf) and then a 1 mL aliquot of culture was centrifuged at 10 000 g for 2 min. The pelleted cells were resuspended with Na-PB (500 μ L) and the cell suspension was subjected to glass bead (30 μ L) disruption for 5 min. Afterward, the cell-free lysate was recovered by centrifugation at 10 000 g for 2 min. To take activity measurements, the cell-free lysate was diluted appropriately to 500 μ L of Na-PB and incubated for 20 min at 37 °C. A 40 μ L aliquot of 4-NPG stock solution (see above) was added to the mix and allowed to react for 15 min at 37 °C. The reaction was stopped by adding a 400 μ L aliquot of 200 mM sodium carbonate, and the absorbance measurement was taken at 405 nm with a UV-vis spectrophotometer. Specific activity calculations were made with *E. coli* K12 β -glucuronidase (Cat. no. 3 707 580 001, Sigma-Aldrich) as the standard using the conversion factor of 398 nmol min⁻¹.

■ ASSOCIATED CONTENT

Supporting Information

The Supporting Information is available free of charge at <https://pubs.acs.org/doi/10.1021/acssynbio.2c00137>.

Plasmids; strains and primers lists; plasmid maps; guidelines on the use of the CRISPR/Cas genome-editing toolbox in *M. maripaludis*; *M. maripaludis* natural transformation protocol; and promoter sequences (PDF)

■ AUTHOR INFORMATION

Corresponding Author

Silvan Scheller – Department of Bioproducts and Biosystems, School of Chemical Engineering, Aalto University, FI-02150 Espoo, Finland; orcid.org/0000-0002-0667-9224; Phone: +358 50 3565 175; Email: silvan.scheller@aalto.fi

Authors

Jichen Bao – Department of Bioproducts and Biosystems, School of Chemical Engineering, Aalto University, FI-02150 Espoo, Finland

Enrique de Dios Mateos – Department of Bioproducts and Biosystems, School of Chemical Engineering, Aalto University, FI-02150 Espoo, Finland

Complete contact information is available at:

<https://pubs.acs.org/doi/10.1021/acssynbio.2c00137>

Author Contributions

J.B. and S.S. conceived the study and wrote the manuscript. J.B. and E.D.M. performed the experiments. All authors commented and approved the final version of the manuscript. All authors declare no conflict of interest.

Notes

The authors declare no competing financial interest.

■ ACKNOWLEDGMENTS

The authors thank the summer laboratory assistants Han Le, An Nguyen, and Pradhuman Jetha for their work on plasmid constructions and *M. maripaludis* transformations. They also kindly thank the following individuals: Prof. Kyle Costa for providing the *M. maripaludis* JJ Δ upt strain and plasmid pLW40, Prof. William B. Whitman for providing plasmids pMEV4 and pMEV4mTs, and the *M. voltae* A3 strain, and Prof. John Leigh and Dr. Thomas Lie for providing the *M.*

maripaludis S2 strain. Prof. Michael Rother, Prof. Qunxin She, Prof. Dipti Nayak, and Dr. Zhe Lyu are acknowledged for their helpful discussions. They are also thankful to Dr. Ingemar von Ossowski, Dr. Norman Adlung, and Dr. Vera Jäger for providing critical and helpful comments on the manuscript. The Novo Nordisk Foundation and the Academy of Finland are acknowledged for funding this study (grant NNF19OC0054329 and grant 326020 to S.S.).

REFERENCES

- (1) Wintsche, B.; Jehmlich, N.; Popp, D.; Harms, H.; Kleinstueber, S. Metabolic adaptation of methanogens in anaerobic digesters upon trace element limitation *Front. Microbiol.*, 2018; Vol. 9, 1–10.
- (2) Braga Nan, L.; Trably, E.; Santa-Catalina, G.; Bernet, N.; Delgenès, J. P.; Escudí, R. Biomethanation processes: new insights on the effect of a high H₂ partial pressure on microbial communities. *Biotechnol. Biofuels* 2020, 13, 1–17.
- (3) Aldridge, J.; Carr, S.; et al. Anaerobic production of isoprene by engineered *Methanosarcina* species Archaea. *Appl. Environ. Microbiol.* 2021, 87, e02417–e02420.
- (4) Lyu, Z.; Jain, R.; Smith, P.; Fetchko, T.; Yan, Y.; Whitman, W. B. Engineering the autotroph *Methanococcus maripaludis* for geraniol production. *ACS Synth. Biol.* 2016, 5, 577–581.
- (5) Simpson, P. G.; Whitman, W. B. Anabolic pathways in methanogens. In *Methanogenesis*; Springer, Boston: MA, 1993; 10.1007/978-1-4615-2391-8_11 pp 445–472.
- (6) Ragsdale, S. W.; Pierce, E. Acetogenesis and the Wood-Ljungdahl pathway of CO₂ fixation. *Biochim. Biophys. Acta, Proteomics* 2008, 1784, 1873–1898.
- (7) Müller, V. New Horizons in acetogenic conversion of one-carbon substrates and biological hydrogen storage. *Trends Biotechnol.* 2019, 37, 1344–1354.
- (8) Lemaire, O. N.; Jespersen, M.; Wagner, T. CO₂ -fixation strategies in energy extremophiles: what can we learn from acetogens? *Front. Microbiol.*, 2020; Vol. 11, 1–8.
- (9) Schöne, C.; Poehlein, A.; Jehmlich, N.; Adlung, N.; Daniel, R.; von Bergen, M.; Scheller, S.; Rother, M. Deconstructing *Methanosarcina acetivorans* into an acetogenic archaeon. *Proc. Natl. Acad. Sci. U.S.A.* 2022, 119, No. e2113853119.
- (10) Haydock, A. K.; Porat, I.; Whitman, W. B.; Leigh, J. A. Continuous culture of *Methanococcus maripaludis* under defined nutrient conditions. *FEMS Microbiol. Lett.* 2004, 238, 85–91.
- (11) Müller, A. L.; Gu, W.; Patsalo, V.; Deutzmann, J. S.; Williamson, J. R.; Spormann, A. M. An alternative resource allocation strategy in the chemolithoautotrophic archaeon *Methanococcus maripaludis*. *Proc. Natl. Acad. Sci. U.S.A.* 2021, 118, No. e2025854118.
- (12) Kessler, P. S.; Daniel, C.; Leigh, J. A. Ammonia switch-off of nitrogen fixation in the methanogenic archaeon *Methanococcus maripaludis*: mechanistic features and requirement for the novel GlnB Homologues, Nif1 and Nif2. *J. Bacteriol.* 2001, 183, 882–889.
- (13) Kessler, P. S.; Leigh, J. A. Genetics of nitrogen regulation in *Methanococcus maripaludis*. *Genetics* 1999, 152, 1343–1351.
- (14) Lie, T. J.; Wood, G. E.; Leigh, J. A. Regulation of *nif* expression in *Methanococcus maripaludis*: roles of the euryarchaeal repressor NrpR, 2-oxoglutarate, and two operators. *J. Biol. Chem.* 2005, 280, 5236–5241.
- (15) Goyal, N.; Zhou, Z.; Karimi, I. A. Metabolic processes of *Methanococcus maripaludis* and potential applications. *Microb. Cell Fact.* 2016, 15, No. 107.
- (16) Lohner, S. T.; Deutzmann, S.; Logan, B. E.; Leigh, J.; Spormann, A. M. Hydrogenase-independent uptake and metabolism of electrons by the archaeon *Methanococcus maripaludis*. *ISME J.* 2014, 8, 1673–1681.
- (17) Moore, B. C.; Leigh, J. A. Markerless mutagenesis in *Methanococcus maripaludis* demonstrates roles for alanine dehydrogenase, alanine racemase, and alanine permease. *J. Bacteriol.* 2005, 187, 972–979.
- (18) Ran, F. A.; Hsu, P. D.; Wright, J.; Agarwala, V.; Scott, D. A.; Zhang, F. Genome engineering using the CRISPR-Cas9 System. *Nat. Protoc.* 2013, 8, 2281–2308.
- (19) Shalem, O.; Sanjana, E. N.; Hartenian, E.; Shi, X.; Scott, D. A.; Mikkelsen, T. S.; Heckl, D.; Ebert, B. L.; Root, D. E.; Doench, J. G.; Zhang, F. Genome-scale CRISPR-Cas9 knockout screening in human cells. *Science* 2014, 343, 84–88.
- (20) Decaestecker, W.; Buono, R. A.; Pfeiffer, M. L.; Vangheluwe, N.; Jourquin, J.; Karimi, M.; van Isterdael, G.; Beeckman, T.; Nowack, M. K.; Jacobs, T. B. CRISPR-Tsko: A technique for efficient mutagenesis in specific cell types, tissues, or organs in Arabidopsis. *Plant Cell* 2019, 31, 2868–2887.
- (21) Miao, J.; Guo, D.; Zhang, J.; Huang, Q.; Qin, G.; Zhang, X.; Wan, J.; Gu, H.; Qu, L. J. Targeted mutagenesis in rice using CRISPR-Cas system. *Cell Res.* 2013, 23, 1233–1236.
- (22) Jessop-Fabre, M. M.; Jakočiūnas, T.; Stovicek, V.; Dai, Z.; Jensen, M. K.; Keasling, J. D.; Borodina, I. EasyClone-MarkerFree: A vector toolkit for marker-less integration of genes into *Saccharomyces cerevisiae* via CRISPR-Cas9. *Biotechnol. J.* 2016, 11, 1110–1117.
- (23) Cai, P.; Duan, X.; Wu, X.; Gao, L.; Ye, M.; Zhou, Y. J. Recombination machinery engineering facilitates metabolic engineering of the industrial yeast *Pichia Pastoris*. *Nucleic Acids Res.* 2021, 49, 7791–7805.
- (24) Gophna, U.; Allers, T.; Marchfelder, A. Finally, archaea get their CRISPR-Cas Toolbox. *Trends Microbiol.* 2017, 25, 430–432.
- (25) Nayak, D. D.; Metcalf, W. W. Cas9-mediated genome editing in the methanogenic archaeon *Methanosarcina acetivorans*. *Proc. Natl. Acad. Sci. U.S.A.* 2017, 114, 2976–2981.
- (26) Zetsche, B.; Gootenberg, J. S.; Abudayyeh, O. O.; Slaymaker, I. M.; Makarova, K. S.; Essletzbichler, P.; Volz, S. E.; Joung, J.; van der Oost, J.; Regev, A.; Koonin, E. V.; Zhang, F. Cpf1 is a single RNA-guided endonuclease of a Class 2 CRISPR-Cas system. *Cell* 2015, 163, 759–771.
- (27) Zetsche, B.; Heidenreich, M.; Mohanraju, P.; Fedorova, I.; Kneppers, J.; DeGennaro, E. M.; Winblad, N.; Choudhury, S. R.; Abudayyeh, O. O.; Gootenberg, J. S.; Wu, W. Y.; Scott, D. A.; Severinov, K.; van der Oost, J.; Zhang, F. Multiplex gene editing by CRISPR–Cpf1 using a single crRNA array. *Nat. Biotechnol.* 2017, 35, 31–34.
- (28) Fonseca, D. R.; Halim, M. F. A.; Holten, M. P.; Costa, K. C. Type IV-like pili facilitate transformation in naturally competent archaea. *J. Bacteriol.* 2020, 202, 1–12.
- (29) Dodsworth, J. A.; Leigh, J. A. Regulation of nitrogenase by 2-oxoglutarate-reversible, direct binding of a PII - like nitrogen sensor protein to dinitrogenase. *Proc. Natl. Acad. Sci. U.S.A.* 2006, 103, 9779–9784.
- (30) White, M. F.; Allers, T. DNA repair in the archaea - an emerging picture. *FEMS Microbiol. Rev.* 2018, 42, 514–526.
- (31) Tumbula, D. L.; Makula, R. A.; Whitman, W. B. Transformation of *Methanococcus maripaludis* and identification of a Pst I-like restriction system. *FEMS Microbiol. Lett.* 1994, 121, 309–314.
- (32) Kohler, P. R. A.; Metcalf, W. W. Genetic manipulation of *Methanosarcina* spp. *Front. Microbiol.* 2012, 3, No. 259.
- (33) Lie, T. J.; Leigh, J. A. A novel repressor of *nif* and *glnA* expression in the methanogenic archaeon *Methanococcus maripaludis*. *Mol. Microbiol.* 2003, 47, 235–246.
- (34) Lie, T. J.; Leigh, J. A. Regulatory response of *Methanococcus maripaludis* to alanine, an intermediate nitrogen source. *J. Bacteriol.* 2002, 184, 5301–5306.
- (35) Lyu, Z.; Chou, C.-W.; Shi, H.; Wang, L.; Ghebream, R.; Phillips, D.; Yan, Y.; Duin, E. C.; Whitman, W. B. Assembly of methyl-coenzyme M reductase in the methanogenic archaeon *Methanococcus maripaludis*. *J. Bacteriol.* 2018, 200, No. e00746-17.
- (36) Lienemann, M.; Deutzmann, J. S.; Milton, R. D.; Sahin, M.; Spormann, A. M. Mediator-free enzymatic electrosynthesis of formate by the *Methanococcus maripaludis* heterodisulfide reductase super-complex. *Bioresour. Technol.* 2018, 254, 278–283.
- (37) Akinyemi, T. S.; Shao, N.; Lyu, Z.; Drake, I. J.; Liu, Y.; Whitman, W. B. Tuning gene expression by phosphate in the

methanogenic archaeon *Methanococcus maripaludis*. *ACS Synth. Biol.* **2021**, *10*, 3028–3039.

(38) Ding, Y.; Berezuk, A.; Khursigara, C. M.; Jarrell, K. F. Bypassing the need for the transcriptional activator EarA through a spontaneous deletion in the BRE portion of the *fla* operon promoter in *Methanococcus maripaludis*. *Front. Microbiol.* **2017**, *8*, No. 1329.

(39) Whitman, W. B.; Shieh, J.; Sohn, S.; Caras, D. S.; Premachandran, U. Isolation and characterization of 22 mesophilic *Methanococci*. *Syst. Appl. Microbiol.* **1986**, *7*, 235–240.

(40) Gibson, D. G.; Young, L.; Chuang, R. Y.; Venter, J. C.; Hutchison, C. A.; Smith, H. O. Enzymatic assembly of DNA molecules up to several hundred kilobases. *Nat. Methods* **2009**, *6*, 343–345.

(41) Labun, K.; Montague, T. G.; Krause, M.; Torres Cleuren, Y. N.; Cleuren, Y. N. T.; Tjeldnes, H.; Valen, E. CHOPCHOP v3: Expanding the CRISPR web toolbox beyond genome editing. *Nucleic Acids Res.* **2019**, *47*, w171–w174.

(42) Long, F.; Wang, L.; Lupa, B.; Whitman, W. B. A flexible system for cultivation of *Methanococcus* and other formate-utilizing methanogens. *Archaea* **2017**, *2017*, No. 7046026.